Short-range structure of Al-Mn and Al-Mn-Si aperiodic alloys

Yanjun Ma and Edward A. Stern
Physics Department, FM-15, University of Washington, Seattle, Washington 98195
(Received 17 February 1988)

X-ray-absorption fine-structure results on the icosahedral Al-Mn and Al-Mn-Si, α-(Al-Mn-Si), and decagonal Al-Mn alloys are presented. High-resolution first-shell Al radial distributions around Mn atoms were obtained using a newly developed, direct Fourier-transform method. The first and second Mn shells are analyzed in detail. The Al and Mn positions on the structural unit of the icosahedral phase are determined from these results. The result is in agreement with the speculation that the structural unit is a Mackay icosahedron (MI). Furthermore, it is found that about 40% of the MI units in the icosahedral phase have the same connection as that in α-(Al-Mn-Si) and the average coordination number of the MI is about 7 in the icosahedral phase. The MI units also closely resemble those in the α phase, including the distortion induced by the cubic packing of the MI's in α-(Al-Mn-Si). These results suggest the presence of a short-range cubic environment in the icosahedral phase with an estimated correlation length of about 20 Å. These results are in disagreement with both the completely random accretion of oriented MI units and a quasicrystalline arrangement of the MI. Results on the decagonal Al-Mn phase and the role of Si in icosahedral Al-Mn-Si are also discussed.

I. INTRODUCTION

Since the discovery of the icosahedral phase (IP) of Al-Mn (Ref. 1) extensive research has been done both experimentally and theoretically to determine the structure of icosahedral Al-Mn and other icosahedral alloys. Yet despite all the effort the question remains as to the position of the atoms in the icosahedral and related noncrystallographic alloys, such as the decagonal alloys.[2]

There are speculations[3,4] that a Mn icosahedron with associated Al atoms [the so-called Mackay icosahedron (MI)] is the structural unit in the icosahedral Al-Mn and Al-Mn-Si. Recent experimental evidence[5] verified the existence of such a structural unit with edge size of 5 Å. Based on this structural unit there exist competing models for the IP. The quasicrystalline (QC) model (e.g., Gratias and Cahn[6]) was initially proposed by Levine and Steinhardt.[7] The randomly connected icosahedra (RCI) model was initially proposed by Shechtman and Blech.[8] Stephens and Goldman[9] have shown that the RCI model gives diffraction peaks with finite width, which provides a natural explanation for the experimental measurements.[10] Using computer simulation, we have shown independently that a face-connected RCI model[11] gives a diffraction pattern similar to that of the experimental ones[10] with center-to-center distance between the icosahedra equal to that in α-(Al-Mn-Si). It has been shown that with the introduction of phason strains the QC model can also give peaks with a finite width.[12] Another class of models is the twinning model.[13] At present these models cannot satisfactorily explain all the experimental results on the icosahedral phase, so the models have been modified to include nonideal packing of the units. Therefore it is important to obtain more information on the connection between the units to distinguish the correct model as well as to identify the complete structural unit in the IP. In this paper we present x-ray-absorption fine-structure (XAFS) results on the local environment around Mn atoms. These results permit us to fill in the Mn skeleton of the icosahedral unit by locating the Al and Si atoms and to give more experimental evidence on the connection between the units.

XAFS measures the local structure around a particular type of atom in a solid.[14] We use the acronym XAFS instead of EXAFS (extended x-ray-absorption fine structure) because for the first coordination shell no multiple-scattering effects occur and it is possible to use the fine structure in the near edge as well as the extended region.[15] XAFS gives the partial radial distribution function (RDF) around a particular type of atom, and, in some cases when multiple scattering is present, information about angles can also be obtained. In this paper we present XAFS studies of i-$Al_{85}Mn_{15}$, i-$Al_{79}Mn_{15.4}Si_{5.6}$, the α phase of $Al_{73}Mn_{16}Si_{11}$, and decagonal $Al_{78}Mn_{22}$ (T phase) alloys at the Mn K edge. We give a detailed analysis of the Mn-Mn scattering[5] which provides information on both the Mn on the MI and the connection between the MI units. We also obtain a first-shell Al RDF for these alloys which reveals fine structure in the distribution. The first-shell result is consistent with the notion that the MI is the structural unit. The MI has a different dimension than the one that has been suggested[4] and is similar to the one in α-(Al-Mn-Si) including distortions of the units. In addition, it is found that about 40% of the MI units in the icosahedral phase have similar connections to those in α-(Al-Mn-Si) and that the MI units closely resemble those in the α phase, including the distortion induced by the cubic packing of the MI, suggesting that to a large degree the packing of the MI in the IP also resembles that in the α phase.

We will briefly describe the experimental measurement in Sec. II. In Sec. III we describe the structure of α-(Al-

Mn-Si) since our analysis is based on a comparison between the XAFS of the IP's and the α phase. We obtain the first-shell RDF for these alloys in Sec. IV. In Sec. V the Mn-Mn shells are discussed. In Sec. VI we discuss these results in terms of the models proposed for the IP. We conclude in Sec. VII.

II. EXPERIMENT

The icosahedral, decagonal, and crystalline samples were made by the usual melt-spun or slow-cooling methods. The aperiodic alloy samples are almost single phase except for the presence of small amounts of fcc Al. However, since more than 95% of the Mn atoms are in the icosahedral or decagonal phase the presence of the Al phase has a negligible effect on the Mn XAFS.

We also annealed the *i*-(Al-Mn-Si) sample for 1 and 44 h in vacuum at 500 °C to study structural changes on annealing. X-ray powder diffraction scans of the 44-h annealed sample showed the patterns of α-(Al-Mn-Si).

The samples were powdered, sieved through 325 or 400 mesh, and rubbed onto the sticky side of Scotch Magic transparent type. 4–8 layers of tape were used to make the absorption step $\Delta\mu x$ at the Mn K edge close to one for transmission measurements. The measurements were done at beamline X-11 of the National Synchrotron Light Source at Brookhaven National Laboratory using a Si(111) double-crystal monochromator. Care was taken to eliminate higher harmonics in the x-ray beam by detuning the monochromator. These precautions helped to minimize distortions of the XAFS signal to below about 5%. The samples were measured at 15 K. Also measured under the same conditions was orthorhombic Al_6Mn, which is used as a standard.

The XAFS data for $\chi=[\mu(E)-\mu_0(E)]/\mu_0(E)$ were extracted from the measured absorption coefficient $\mu(E)$ by the usual method[14] of normalization and subtraction of the smoothly varying background, $\mu_0(E)$. The data were converted to k space using $\hbar^2k^2/2m=E-E_0$ where the energy origin E_0 was chosen so that the half maximum of the edge equals the Fermi energy calculated by assuming a free-electron gas for the conduction electrons.

In Fig. 1 we plot a sampling of the $\chi(k)$ data for the samples. The $\chi(k)$ data for the α phase and *i*-(Al-Mn-Si) were previously published[5] and are not given here. Note that the signal-to-noise ratio for the Al-Mn-Si sample is good till about $k=14$ Å^{-1}, for the *i*-(Al-Mn) sample till 11–12 Å^{-1}, but for the *T*-(Al-Mn) sample only to 9–10 Å^{-1}. This indicates a larger disorder for the *T*-phase sample.

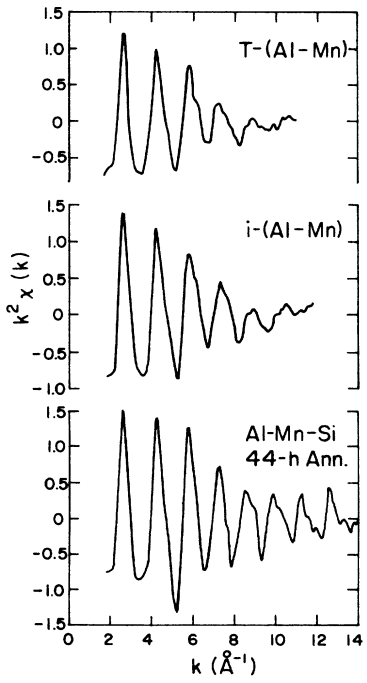

FIG. 1. $k^2\chi(k)$ for the *i*-(Al-Mn), 44-h annealed Al-Mn-Si, and the decagonal sample, *T*-(Al-Mn), at 15 K.

III. STRUCTURE OF α-(Al-Mn-Si)

In this section we describe the structure of α-(Al-Mn-Si).[16] In the following we treat Si the same as Al since they are so close together on the Periodic Table that it is not possible to distinguish them experimentally. Neglecting Al atoms, the unit cell of the α phase is shown in Fig. 2. The structure is an approximately bcc packing of icosahedra with Mn at the vertices. However, the icosahedron at the center of the unit cell is somewhat different from that at the corners, reducing the structure to simple cubic. There are two different Mn sites corresponding to each type of icosahedron. The type-1 Mn icosahedron has two different edge dimensions, six of 5.08 Å which are parallel to the cubic axes and 24 of 5.12 Å, giving an average edge length of 5.11 Å. Similarly, the type-2 icosahedron has six of 4.85 Å and 24 of 5.00 Å, giving an average edge length of 4.97 Å.

The icosahedra all have the same orientation. They connect through a distorted octahedron of Mn atoms whose opposite faces are the faces of the connecting icosahedra. Figure 3 shows such a connection between two Mn faces with the inclusion of the Al atoms in between. There are nine different Al sites in the structure.

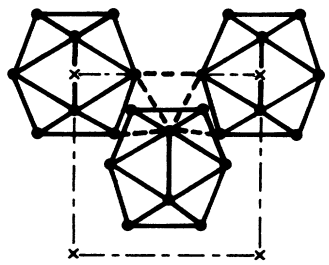

FIG. 2. Unit cell for the α phase, viewing along a [100] axis. For clarity only three Mn icosahedra are shown. Only Mn atoms are shown. The cubic edge is 12.68 Å. The center icosahedron is different from the icosahedra at the corners. The average edge length of the icosahedron is 5.04 Å and the dashed lines average 4.46 Å.

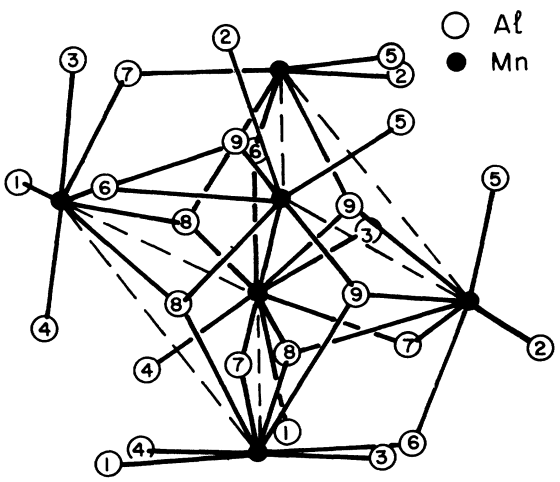

FIG. 3. The connection region between two neighboring Mn icosahedra with Al atoms shown. Only one triangular face of each icosahedron is shown and is indicated by the dashed line. Only Mn-Al bonds which are shorter than 3.2 Å are drawn. The labeling of the Al atoms follows that of Ref. 15.

In Table I we list all the nearest-neighbor Al atoms, and the first two nearest Mn neighbor shells of the two Mn sites with their positions relative to the Mn icosahedron.

To summarize, the Al nearest neighbors of the Mn atoms form two groups; one [Al(1), Al(2), Al(4), Al(5), Al(8), Al(9)] together with the Mn icosahedra forms the Mackay icosahedra[4] and the other group consists of the Al atoms between the connecting MI units [Al(3), Al(6), Al(7)] (which have been referred to as the "glue" atoms[4]). Note that the octahedron bond between two MI units is also supported by Al octahedra, formed by the Al atoms on the surface of the MI, and the Al connecting atoms Al(6,7). The connecting atoms are shared by two such bonds. Thus the stability of the bonds is correlated through the connecting atoms. All of the Al atoms have Al-Mn distances less than 2.85 Å. In addition there are two longer distances of 2.96 and 3.07 Å which are from Mn atoms on one MI to Al on the neighboring MI. Note that the distances of the two Mn-Al groups overlap except for the two longer Mn-Al distances. In contrast the Mn-Mn distances can be divided in two distinguishable groups, namely, five Mn-Mn distances of ~ 5 Å which are along the edges of the Mn icosahedra, and five Mn-Mn at ~ 4.5 Å which are between the Mn icosahedra. These distances are indicated in Fig. 2 by the solid and dashed lines, respectively. We used this fortunate fact as our basis of identification of the structural unit in a previous publication.[5] Further details are presented in Sec. V.

The distortion of the MI units can be attributed to the bcc packing in α-(Al-Mn-Si). The shorter edges of the Mn icosahedra are parallel to the cubic unit-cell edge and do not participate in the octahedron bonding between two MI units. Furthermore, associated with the extreme short edge of 4.85 Å is a lack of the equivalent Al(3) atoms for the type-2 Mn icosahedron. It has been suggested[17] that the packing arrangement of the MI units does not leave room for the equivalent of the Al(3) atoms to squeeze onto the type-2 MI. This makes the type-2 MI lose its icosahedral symmetry around the extreme short edge, in distinction to the type-1 icosahedron where all edges have a similar distribution of Al atoms at the distance of the Al(3) sites from the MI center.

We also note that Al(1),Al(8) and Al(2),Al(9) are almost collinear with the edge of the Mn icosahedron. The aver-

TABLE I. Al and Mn neighbors of Mn atoms in α-(Al-Mn-Si), according to Ref. 15. The Mn-Mn distances given are up to 5.5 Å and Mn-Al are up to 3.5 Å. The adjusted Mn-Al distances are given in parentheses. Figure 3 can be consulted for visualization.

Mn(1)			Mn(2)			
Number of neighbors	Type[a]	Distance (Å)	Number of neighbors	Type[a]	Distance (Å)	Position[b]
1	Al(1)	2.58	1	Al(2)	2.53	Near center of edge
1	Al(4)	2.43(2.39)	1	Al(5)	2.27(2.38)	Inside
1	Al(6)	2.57	2	Al(6)	2.60	Between
2	Al(7)	2.84(2.70)	1	Al(7)	2.53	Between
2	Al(8)	2.61	2	Al(9)	2.59	Near center of edge
2	Al(8)	2.64	2	Al(9)	2.62	Near center of edge
2	Al(9)	2.96(2.92)	2	Al(8)	3.07	On neighbor MI
1	Al(3)	2.46				Between
1	Mn(1)	4.38	1	Mn(2)	4.55	On neighbor MI
2	Mn(2)	4.43	2	Mn(1)	4.43	On neighbor MI
2	Mn(2)	4.49	2	Mn(1)	4.49	On neighbor MI
1	Mn(1)	5.08	1	Mn(2)	4.85	On same MI
4	Mn(1)	5.12	4	Mn(2)	5.00	On same MI

[a] With the notation of Ref. 15.

[b] Relative to Mn icosahedron. For example, *between* in the "position" column means that the Al atoms are positioned between two Mn icosahedra; *inside* means between the Mn atom and the center of the icosahedron; *near center of edge* means that the Al atom is near the center of the edge of the Mn icosahedron.

aged angle between Mn-Al and the edge of the icosahedron is approximately 14°. This angle is small enough to cause significant multiple-scattering effects (the focusing effect[18]) on the XAFS of the Mn-Mn scattering (the 5-Å distance) by the intervening Al atom. No Al atoms are expected to have a significant focusing effect on the XAFS of the Mn-Mn along the edges (~ 4.5 Å) of the octahedron connecting the icosahedra (the averaged angle is about 33°).

We suspect that there are more uncertainties in the x-ray diffraction determination of the Mn-Al distances than the stated 0.03 Å.[16] An example is the abnormally short 2.27-Å Mn-Al distance from Al(5) inside the Mn(2) icosahedron to the Mn(2) atom on the vertex. Here the smaller Mn(2) icosahedron has an enclosed Al icosahedron which is bigger than the Al icosahedron enclosed by the bigger Mn(1) icosahedron, causing the suspiciously short 2.27 distance.

XAFS measurements give information about both the Mn-Al and the Mn-Mn structure changes in the IP compared with the α phase. This is the subject of the following two sections.

IV. RADIAL DISTRIBUTION FUNCTIONS

In this section we discuss the Mn-Al radial distribution function in the icosahedral phase and compare it with that of the α phase. To obtain the Al RDF we use a newly developed analysis technique which has been described elsewhere.[15] Here we only briefly describe the procedure.

Starting with the $\chi(k)$ data given before, we obtain the usual Fourier transforms $[\mathcal{F}(r)]$ of the $\chi(k)$ data as shown in Fig. 4 and back transform to k space to obtain the single-shell contribution to $\chi(k)$ by use of an r-space window from 1.4 to 2.7 Å. This covers the real distances from about 1.9 to 3.2 Å. We then take the ratio of the amplitudes and the difference in phases with that of the standard, namely, first shell about Mn of Al_6Mn which has a known structure,[19] to eliminate the atomic backscattering amplitude and phase from $\chi(k)$. Next we correct for the structure of Al_6Mn to obtain the reduced $\chi''(k)$ which depends only on the Mn-Al pair distribution function of the unknown sample. However, since the experimental data are only available over a finite k range, in our case from about 2.4 to 12 $Å^{-1}$ (to about 10 $Å^{-1}$ for the decagonal Al-Mn), we recover the low k data by extrapolating down to $k=0$ using the cumulant expansion and we cut off the noisy high k data by a convergence factor $e^{-2k^2\sigma_c^2}$. Figure 5 gives an example of the amplitude and the phase of $\chi''(k)$ for i-(Al-Mn-Si) after correcting for the structure of Al_6Mn and the extrapolation using the cumulant expansion.

It should be emphasized that this method has two distinctive advantages over the more standard method of fitting a model to the data. The result is not biased by the assumed form of the model and the spatial resolution is not limited by the restrictions of the model.

The reduced $\chi''(k)$ is multiplied by a convergence factor, Fourier transformed to r space and multiplied by the factor $r^2e^{2r/\lambda}$ to obtain the RDF as shown in Fig. 6. The resolution is dominated by $\sigma_c^2=0.004$ $Å^2$, so that the resolution is about 0.065 Å. For the decagonal Al-Mn no convergence factor was needed because the data decay rapidly at high k, but, in order to compare with other samples, the same convergence factor was still used. The error bars in the plot are obtained by analyzing different experimental scans separately and is an indication of the errors due to the experimental and also to analysis variations such as different isolation window sizes. However, there are possible additional errors which do not appear as variations by such an analysis, e.g., any errors introduced by the Al_6Mn standard will be reproduced in all the results. Many of the systematic errors are present at high k and are minimized by the convergence factor. To compare, Fig. 6 also shows the simulated RDF for the α phase [in Fig. 6(a)] and for Al_6Mn [in Fig. 6(c)] obtained by constructing the reduced $\chi''(k)$ using the structure determined from x-ray diffraction and then Fourier transforming the same way as we did for the experimental data. We see that the experimental RDF of the α phase agrees well qualitatively with that of the simulated α phase. However, there are some significant differences on both sides of the main peak. In particular, the shoulder at about 2.27 Å is shifted to about 2.38 Å and is enhanced. In Sec. III we have pointed out that there might be some errors in the x-ray determination of the

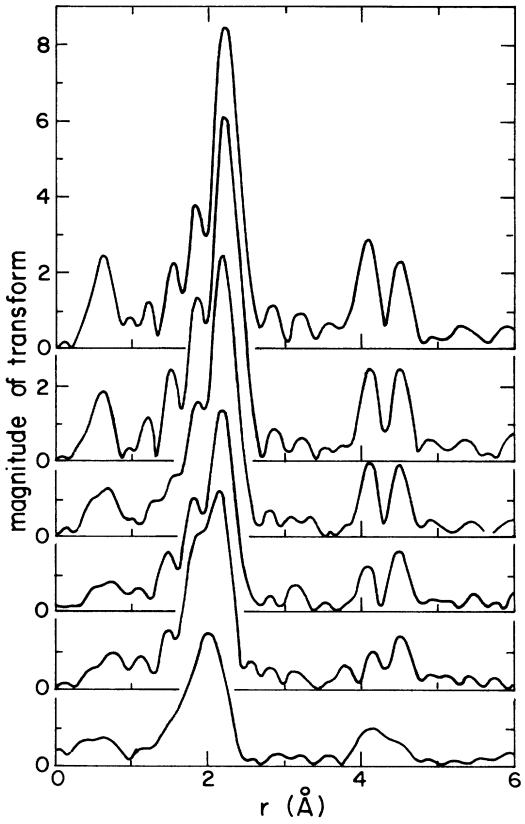

FIG. 4. The magnitude of the Fourier transforms of the $k^3\chi(k)$ data, from top to bottom: α-(Al-Mn-Si), 44-h anneal Al-Mn-Si, 1h anneal Al-Mn-Si, i-(Al-Mn-Si), i-(Al-Mn), and T-(Al-Mn). The transforms are for $2.3 < k < 14$ Å for all the samples except for the decagonal Al-Mn, for which $2.3 < k \lesssim 11$ Å.

anomalously short Mn-Al distances in the α phase. We thus tried to vary the Mn-Al distances of the α phase to get a better agreement between the simulated RDF with that of the experimental one. In doing so we only vary the Mn-Al distances in Table I which are abnormally short or long, namely, Mn(2)-Al(5), Mn(1)-Al(4) and Mn(1)-Al(7), and Mn(1)-Al(9). The fitted RDF is shown in Fig. 6(a) and the new distances are listed in Table I in parentheses. The changes make the two different MI's more similar to one another.

From the area under the RDF which gives the total number of nearest neighbors we find that the coordina-

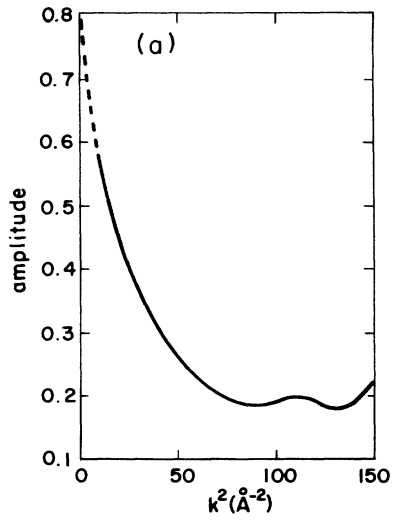

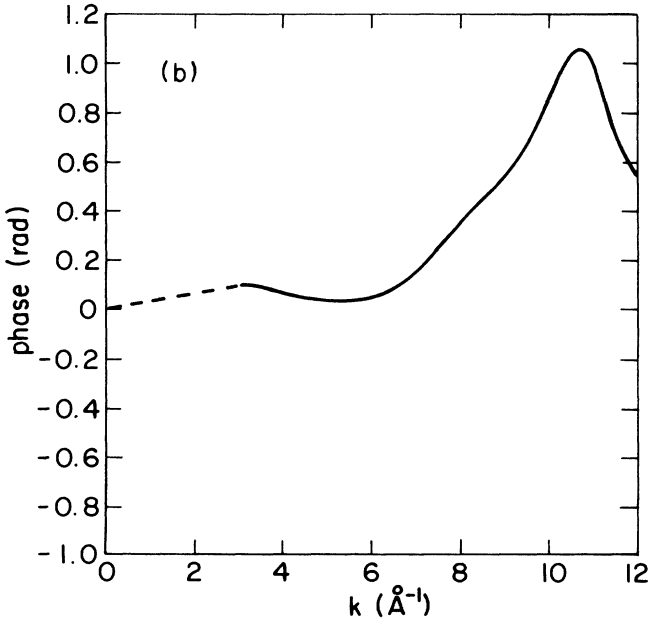

FIG. 5. The amplitude (a) and phase (b) of the corrected $\chi''(k)$ for i-(Al-Mn-Si). The dashed lines show the extrapolation using the cumulant expansion down to $k=0$. A linear term has been subtracted from the phase.

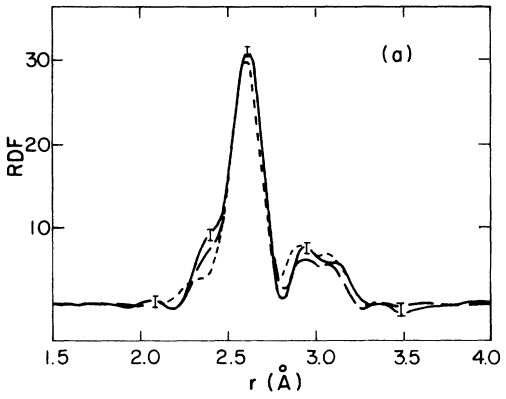

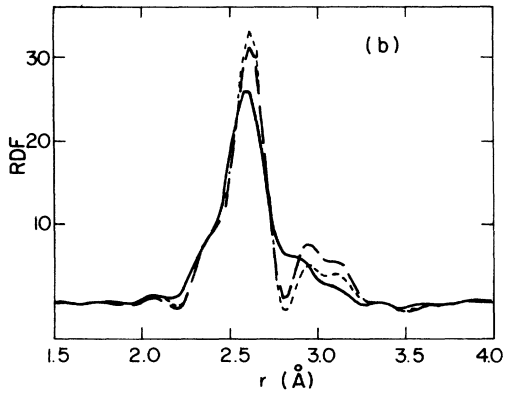

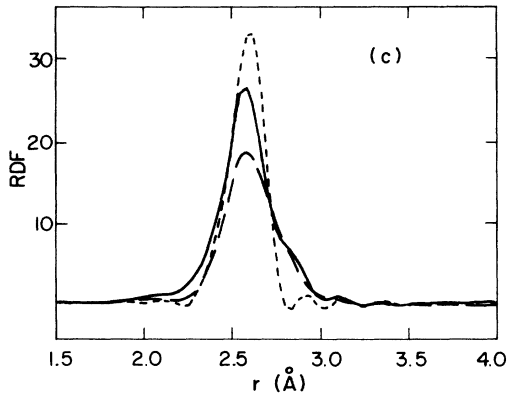

FIG. 6. The RDF's. (a) α-(Al-Mn-Si) simulated using the original Mn-Al distances of Ref. 15 (short-dashed) and the adjusted distances given in Table I (long-dashed), and experimental (solid). (b) The experimental α-(Al-Mn-Si) (long-dashed), the 44-h annealed (short-dashed), and the i-(Al-Mn-Si) (solid). (c): i-(Al-Mn) (solid), decagonal Al-Mn (long-dashed), and Al_6Mn (short-dashed) simulated using Mn-Al distances given by Ref. 16. The RDF's are all broadened by a convergence factor of $e^{-2k^2\sigma^2}$ with $\sigma^2=0.004$ Å^2.

tion number for i-(Al-Mn) is 9.7, i-(Al-Mn-Si) 10.5, and T-(Al-Mn) only 8.5 with an uncertainty of about one in each case. These are all less than the 11.5 of the α phase. Our result for i-(Al-Mn) is consistent with all the previous XAFS measurements[20–24] which found a value of 10. The area is proportional to the intercept of the amplitude at $k=0$. By fixing the intercept to different values within the uncertainties, the area varies but the shape of the RDF shows little change. Since the intercept is obtained from the cumulant expression extrapolation it depends critically on the data at the lower k range. We estimate in this way that the uncertainty in determining the coordination number in this manner is about one atom.

We find no trace of Mn atoms in the first-shell XAFS of all the samples. If there were, it would show up in both the amplitude and the phase of the XAFS. In particular, the effect of the Mn scattering will not be canceled out completely in the ratioing with Al_6Mn which contains only Al backscatters, resulting in negative values in the RDF which are not seen. According to theoretical calculation of Teo and Lee,[25] the backscattering amplitudes $B(k)$ and phases $\delta(k)$ of Mn and Al are very different; the $B(k)$ of Al peaks near $k=0$ while that of Mn tends to zero near $k=0$, and their phases differ by about π. We have done a simulation using the theoretical amplitude and phase[25] and find that replacing one Al atom by one Mn atom indeed causes significant changes in the natural logarithm of the ratio plot and in the phase, which are not seen.

V. Mn-Mn SHELLS

It is clear in the Fourier transform of Fig. 4 that the second and third peak (at ≈ 4 and 4.5 Å, respectively) are very similar in the transform of i(Al-Mn-Si) and α-(Al-Mn-Si). The main difference is that the relative heights of these two peaks change from the α phase to the IP. We know from Sec. III that there are different groups of Mn atoms at these distances, one at 4.5 Å which measures the edge of the Mn-Mn icosahedron and the other at 4 Å which measures the Mn-Mn between the icosahedra. Analysis of the k dependence of the peaks indicates that they are mainly from Mn-Mn scattering. This is not surprising since the Al atoms form a broad distribution at this range, and also the Mn atoms backscatter more strongly at high k (the backscattering amplitude of Mn being more than twice that of the Al atom).

Comparing the transformations of i-(Al-Mn-Si), the annealed samples, and α-(Al-Mn-Si), one notices the monotonic change of the peak heights. In particular, the peak at about 4 Å changes more than the peak at ≈ 4.5 Å. As pointed out previously,[5] the relatively greater rigidity of the more distant peak is very unusual. Taking into account the ≈ 0.5-Å shift due to the scattering phase shift, these two peaks correspond to real distances of 4.5 and 5 Å. Recalling the relation of these two peaks to the structure of the α phase described in Sec. III, the larger change between the α phase and the IP is occurring in the connection between the icosahedra, while the Mn icosahedra themselves remain more rigid in the IP.

To investigate this quantitatively, we use the ratio method. The two peaks are isolated using Fourier filtering and backtransformed into k space. Then the natural logarithm of the ratio of the amplitudes (A_1 and A_α) and the difference in phase between the unknown samples and the α phase are taken. The results are plotted in Figs. 7 and 8, for the second and third shells, respectively.

To interpret ln-(A_1/A_α) and phase-difference results in terms of cumulants of the Mn-Mn radial distribution function it is necessary to show, in addition to no significant Al contribution, that multiple-scattering (MS) effects do not invalidate the interpretation. The MS effects can be divided into two types,[26] MS I and MS II. The MS II effect has large-angle scatterings of the photoelectron at intermediate atoms, while the MS I effect has only small-angle scattering at intermediate atoms, the focusing effect. Thus the near collinearity of Al between Mn-Mn pairs in the third shell contributes a MS I effect. Generally, MS II effects give negligibly small contribu-

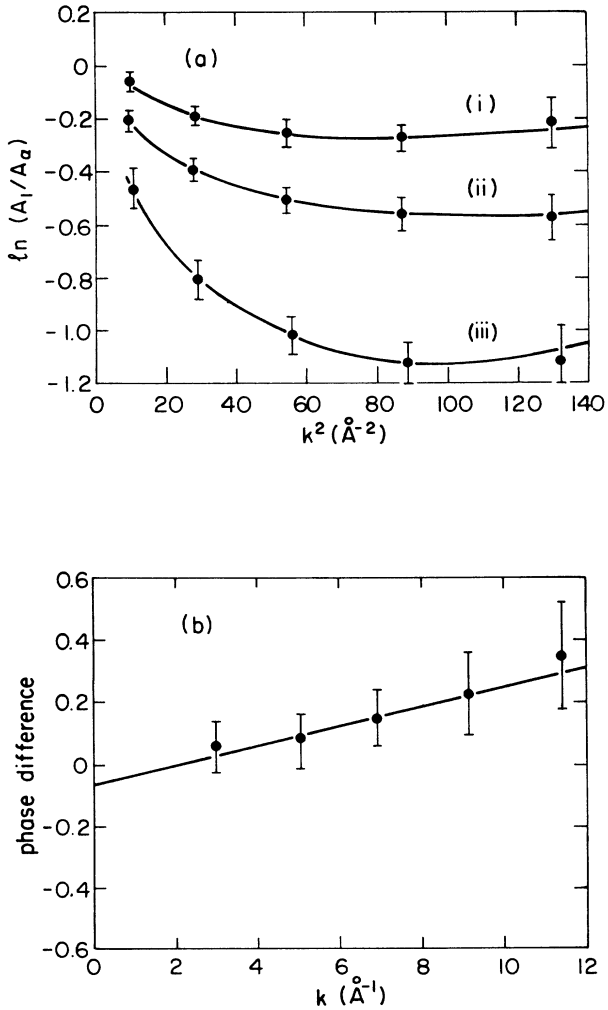

FIG. 7. (a) The natural logarithm of the amplitude ratio for the second shell between the α phase and the 44-h annealed (curve i), 1-h annealed (curve ii) and the i-(Al-Mn-Si) (curve iii). (b) The phase difference (rad) between the IP and the α phase.

tions to the EXAFS. In our case, any MS effect at the two Mn-Mn peaks would have to come from Al intermediate atoms as the nearest MS effects from intermediate Mn atoms would occur at $\sim 4.8 \times 1.5 = 7.2$ Å. For MS II effects the intermediate Al atom would contribute a k dependence to its contribution similar to that of an Al backscatter, which is not seen, in agreement with the expected small MS II effects. However, MS I effects contribute a large effect on the third shell and it is necessary to show that, in spite of this, the change in the RDF as determined from $\ln(A_1/A_\alpha)$ and the phase difference is not affected in the case at hand.

To estimate the focusing effect of the intervening Al atoms for the third shell a calculation was performed which included spherical wave effects[27] (Mustre and Rehr). The dashed lines in Fig. 8 show the calculated amplitude and phase expected for a 0.5° change in the angle between Mn-Al and Mn-Mn. To obtain these curves, the theoretical calculations were used to simulate the third-shell contribution to the XAFS, then Fourier transformed into r space and backtransformed into k space using the same r-space window as used on the experimental data so as to contain the same window effects. It is clear from the phase Fig. 8(b) that any change in the angle must be within 1° since the deviations of these curves from a horizontal line passing through the origin are proportional to the angle change. Thus the MS I effect does not appreciably change between the α phase and IP and the $\ln(A_1/A_\alpha)$ variation displayed in Fig. 8(a) can be interpreted by the usual analysis neglecting MS effects.

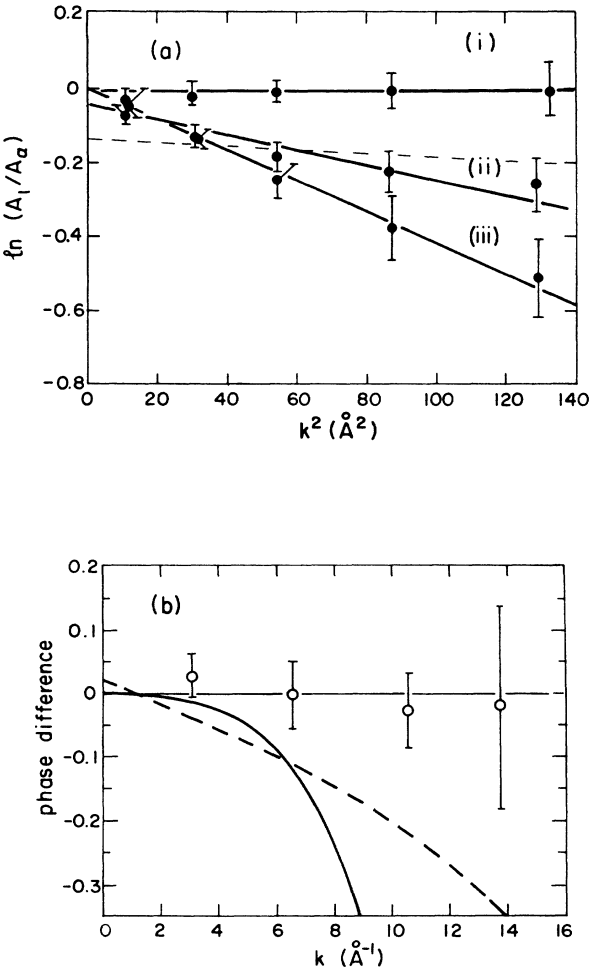

FIG. 8. (a) The natural logarithm of the amplitude ratio for the third shell between the 44-h annealed (curve i), 1-h annealed (curve ii) and the i-(Al-Mn-Si) (curve iii) and the α phase. (b) The phase difference (rad) between the IP and the α phase. The dashed lines show the effect of changing the angle, as explained in the text.

These $\ln(A_1/A_\alpha)$ curves of Fig. 8(a) are approximately straight lines with decreasing slope as we go from as-spun i-(Al-Mn-Si) to the 44-h annealed sample. The intercepts at $k=0$ are all close to the origin within the uncertainty of 5%, indicating no significant change in Mn-Mn neighbors for this peak. Thus the various phases differ only by an approximate Gaussian disorder in the third shell. This not only means that in the various phases are there the same number of Mn atoms at the same distances as in the α phase but the intervening Al atoms [Al(1),Al(8) and Al(2),Al(9)] remain at their same positions relative to the Mn atoms within the uncertainty of about one degree. The latter conclusion follows from the above discussion of the focusing effect. Since the straight line ratio and zero intercept show that no change in the focusing effects has occurred, we conclude that Mn icosahedra with Al atoms near the edges as in α-(Al-Mn-Si) occur in the 44-h annealed sample, in the 1-h annealed sample and in the i-(Al-Mn-Si). However, the finite slope indicates that the Mn-Mn distribution is more disordered by a Debye-Waller factor $\Delta\sigma^2$. For the 1-h annealed sample $\Delta\sigma^2 = 0.0013(5)$ and for the i-(Al-Mn-Si)$=0.0021(6)$ Å^2, indicating that the Mn icosahedra are slightly more distorted than the ones in the α phase.

The phase difference for the third shell between the α and the IP is shown in Fig. 8(b). It is consistent with zero change in average distance within the uncertainty of about 0.02 Å. The 1- and 44-h annealed samples show similar results.

While the phase differences for the second shells are also straight lines as shown in Fig. 7(b), indicating an increase in the average distance in the IP of 0.015(20) Å, the natural logarithm of the ratios of the second peak in Fig. 7(a) are not straight lines. This indicates the disorder is more complicated than a simple Gaussian. However, similar to the behavior of the third-shell ratio, we note that the second shells are also approaching that of the α phase as we anneal the i-(Al-Mn-Si). The second shell of the 44-h annealed sample is almost the same as that of the α phase but the deviation is still nonlinear. There are at least two possible causes for the nonlinear behavior. One explanation is that while Al atoms contribute little to the second shell in the α phase because of their broad distribution, Al atoms could have a different distribution in the IP. This can occur in two ways: Al atoms could rearrange to have a much narrower distribution at this distance or become more collinear with Mn-Mn, thereby contributing more significantly to the second-shell signal

at low k. The other explanation is that the Al atoms do not contribute to the signal at all and that the nonlinear behavior is caused by the non-Gaussian distribution of the Mn-Mn distances in the IP. The behavior of the XAFS phase differences and the ratio of the amplitudes in Figs. 7(a) and 7(b) indicate that the first explanation is unlikely. If the Al atoms contribute substantially in the IP their contribution in both cases discussed above would be greatest at low k. In the case that they bunch up, their contribution would subtract from that of the Mn at low k since the $\delta(k)$ of Al is about π out of phase with that of Mn at low k. In that case the amplitude would drop at low k and the phase would not intercept through the origin in disagreement with the observed behavior. Similarly an appearance of the focusing effect would substantially change the phase, which does not occur in Fig. 7(c). Thus the experimental analysis favors the second explanation, that Mn atoms dominate the second shell.

Because only Mn atoms contribute to the second shell, we can use the same technique to determine the RDF of the Mn atoms in the second peak as was done for the first shell in Sec. III. We use the second shell of α-(Al-Mn-Si) as the standard. The result is shown in Fig. 9 where the r window used is 3.7–4.3 Å, i.e., about 4.2–4.8 Å in real distance. The RDF shows a sharp peak superimposed on a broader background. It appears that the distribution is broader than the range and is cut off at the boundaries. The data outside the range 4.2–4.8 Å are due to the leakage from the main peak even though the data do not cover that range. Note that the RDF is all positive. This is further confirmation that only Mn atoms contribute to the second shell because when a shell is a mixture of different atoms the RDF's obtained by the method of Sec. III usually have negative, unphysical values, an indication that the backscattering amplitudes and phase did not cancel out.[15] The extrapolation of the plot of $\ln(A_1/A_\alpha)$ to $k=0$ give 4.5 ± 0.75 Mn atoms for the second shell.

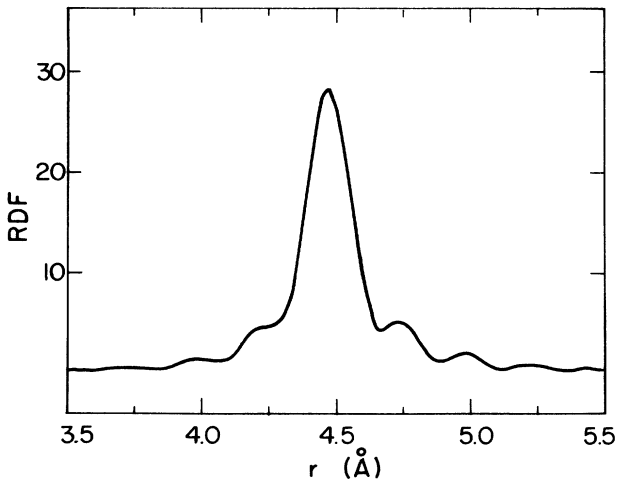

FIG. 9. The RDF for the second shell (Mn-Mn) of i-(Al-Mn-Si) using the second shell of α-(Al-Mn-Si) as a standard. No convergence factor is used.

VI. DISCUSSION

We have shown that the XAFS spectrum for the icosahedral Al-Mn-Si is related to that of the α phase and it approaches that of the α phase upon annealing. In particular, the evidence is quite clear that MI of average edge size about 5.04(3) Å are the structural units in the i-(Al-Mn-Si) with Mn atoms at the vertices. Furthermore it is shown through the focusing effect that the Al atoms sit slightly above the center of the Mn icosahedron edges, making an angle between Mn-Al and Mn-Mn of 14(1)°. These results are obtained directly by comparison between the third shells of the IP and α phase. In the α phase there are smaller Al icosahedra of edge size ≈ 2.55 Å completely enclosed by the Mn icosahedra. Since the Mn icosahedra are so rigid in going from the α phase to the IP it is reasonable to assume that the enclosed Al icosahedra are also present in the IP without significant distortion. As will be discussed below, the first-shell RDF results support such a conclusion. Therefore we reach the conclusion that the average size of the MI in the crystalline α-(Al-Mn-Si) is the same as that in the i-(Al-Mn-Si) phase. The average MI has a somewhat different dimension from the one proposed previously.[4] Our unit is a near sphere of radius 4.8 Å with 12 Mn and 30 Al atoms on the surface and 12 Al atoms radially below the Mn atoms with a Mn-Al distance of approximately 2.4 Å. A portion of the unit is shown in Fig. 11. The Mn atoms are at the vertices of an icosahedron while the 30 Al atoms are along directions from the center of the icosahedron to the bisection of the edges of the icosahedron. There are remaining Al atoms between the MI's and they are at different positions in the two phases since the MI's pack differently. We will discuss this point later.

Since we found that the third shell has a coordination number of 5.0(3) we conclude that, just as in the α phase, two Mn icosahedra cannot touch each other in the IP, i.e., do not share one or more vertices, since touching will increase the coordination number. It is reasonable to assume that in the IP these MI are connected the same way as in the α phase, i.e., through icosahedral faces.

In the α phase each MI connects to eight neighbors, i.e., the maximum allowed without overlapping, along the [111] axes. It is clear from the $\ln(A_1/A_\alpha)$ of the second shell in Sec. V that the connections between the MI's change. In fact the $\ln(A_1/A_\alpha)$ and RDF of Mn atoms on the neighboring unit obtained in Sec. V show two kinds of behavior, a sharp peak superimposed on a broader background. The sharp peak comes from the Mn atoms which have the same distribution in the IP as in the α phase. The broader distribution indicates that the rest of the neighbors of Mn atoms are more disordered in the IP. The total number of Mn atoms at 4.5 Å is obtained by extrapolating to $k=0$, which indicates a 10 ± 15 % decrease in number from the α phase. This can be roughly translated to obtain a coordination number of 7.2 ± 1.2 for the MI unit in the IP. The distribution suggests that a portion [about $\frac{3}{7}$, estimated from Fig. 7(a)] of the MI units in the IP are connected as in the α phase while the majority of the connections are disordered.

This change in the connections between the MI's is also shown by the results of the RDF of Sec. IV. Comparing the RDF of α-(Al-Mn-Si) with that of the i-(Al-Mn-Si) [in Fig. 6(b)] we notice that the small double peaks at around 3 and 3.1 Å are decreased. In Fig. 10 we plotted the difference between the RDF of i-(Al-Mn-Si) and $\frac{3}{8}$ of the RDF of α-(Al-Mn-Si). This number agrees with the number estimated from the second-shell analysis within our experimental error. As can be seen the double peak is well eliminated. Since these distances are from Mn atoms on one MI to the Al atoms on the neighboring MI this result indicates that a portion of the first shell remains the same as in the α phase while the rest is disordered. This is consistent with the second-shell result discussed in the preceding paragraph which indicates that about $40\pm10\%$ [estimated from the $\ln(A_1/A_\alpha)$ and RDF results] of the Mn-Mn connection remain rigid while the rest is disordered.

On the other hand, the main peak position and the shoulder at about 2.38 Å in the RDF's occur for both the IP and the α phase. The shoulder is the same in the two phases except for some smearing in the IP. The main peak height is decreased and broadened in the IP. Recall that in the α phase the smallest distances which cause the shoulder are from Mn atoms to the Al atoms inside the Mn icosahedron. The similarity of the shoulder in the two phases gives direct evidence for the rigidity of the Al icosahedron inside the Mn icosahedron in the IP. Furthermore, the main peak at around 2.6 Å is due to the Al atoms near the center of the edges of the Mn icosahedra and the Al atoms between the Mn icosahedra. The change in the main peak in the IP is consistent with the rigidity of the MI and the disordering of their connections since it contains both types of Al atoms.

The small difference in the MI units between the α phase and the IP raises the question of whether the distortions of the unit in the α phase remain in the IP. As mentioned in Sec. III, the distortions manifest themselves in two different ways. One is to make the dimension of the MI in the center of the cubic unit cell different than that at the corner. The other is to shorten the edge of the MI parallel to the cubic axes. The latter distortion introduces a negative third moment to the radial pair distribution function of the third shell with the largest contribution coming from the 4.85-Å edge. We will now show that our results on the third shell in Fig. 8 indicate that the distortion of the MI unit persists in the IP. If the distortion did not occur so that all edges are equivalent we expect a symmetric distribution or a distribution with a positive third moment, since disorder typically produces a positive third moment because the interatomic potential is asymmetrical in that direction. Thus a lower limit to the expected change in the third moment between a local icosahedral symmetry and the α phase is given by assuming a symmetric distribution of edge dimensions. Since the phase difference is sensitive to changes in odd moments of the distribution, while the $\ln(A_1/A_\alpha)$ is sensitive to only even moments,[14] comparison of the phase must be made to detect change in the third moment. In Fig. 8(b) the expected phase difference, if the third moment disappeared, is plotted as the thick solid line. The measurements are consistent with no change in the third moment within an uncertainty of about 10%, indicating no change in the distortion.

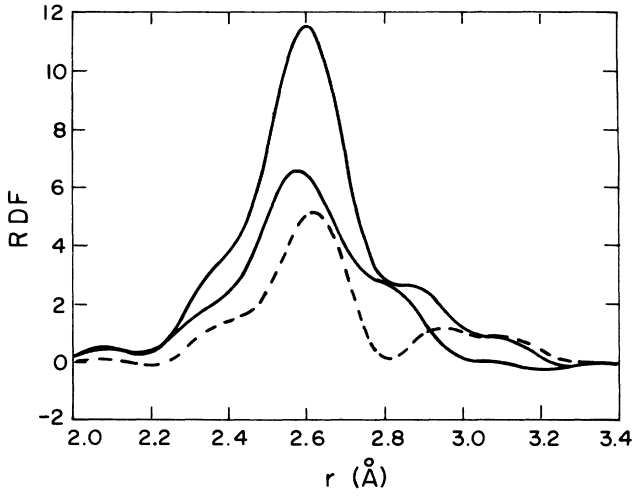

FIG. 10. The RDF's of α-(Al-Mn-Si), i-(Al-Mn-Si), and the difference between that of i-(Al-Mn-Si) and $\frac{3}{8}$ that of the α phase.

As discussed in Sec. III, the distortion of the MI units is due to the packing arrangement of the units, which requires a correlation between three or more units. The preservation of the distortion in the IP indicates that not only the MI unit itself and its connections are similar, but also the correlations between three or more units are similar to the α phase. This interpretation has been discussed in a previous publication.[28]

The preservation of three or more unit correlations in the IP is also supported by the result on the second shell. As discussed previously, we found that about 40% of the connections between MI's in the IP are undisturbed from those of α-(Al-Mn-Si). As noted in Fig. 3 the bonds between the MI units are correlated through sharing the connecting atoms in the α phase. That is, the bond between the MI in the center of the cube and the MI on the [111] direction is affected by the bonds along the three neighboring [111] directions. So the result that about 40% of the bonds are unaffected going from the α phase to the IP strongly suggests that a large portion of the MI's in the IP have a local cubic environment. Further support for this result comes from the presence of an average of about 7 MI neighboring units. By fluctuations a significant number of MI units must have the maximum allowed eight neighbors to obtain such an average. Eight neighbors can only occur by the cubic arrangement along the [111] directions.

We can roughly estimate the cubic correlation length. Assume that about 40% of the units are in the interior of the cubic regions and the rest, the more disordered portion, come from the intergranular region. Further assume that in the interior of the cubic regions each MI has 8 MI neighbors, in the boundary region 6.6 neighbors with 4 of the 6.6 in the interior while 2.6 are on the outside. Such a distribution will give the correct average number of neighbors. Let the cubic regions have average

dimension la, where $a=12.68$ Å is the unit-cell dimension of the α phase. The number of MI's in this region is then $2l^3$, of which approximately $6l^2$ are on the surface. We then have the ratio of surface bonds to bulk bonds as $0.6/0.4=(2.6\times 6l^2)/8(2l^3-6l^2)$, from which we get $l\approx 3.5$. Therefore the average size of the cubic region is about 40 Å and correlation length is of ~ 20 Å. We note the size from this crude estimate is smaller than what can be detected by high-resolution electron microscope.[29]

We now discuss the results of the 44-h annealed IP. This is a crystallized, slightly defective α phase. The composition is somewhat off that of the α phase. From the RDF and Mn-Mn shell results we see that the results are quite close to those of the α phase. The main difference is the second shell and the RDF peak at around 3 Å. Both of them relate to the connection of the MI units. The results are clear evidence again for the relative rigidity of the MI's compared to their interconnections and suggest that increasing Si content has an effect on the connection between the MI units.

The RDF in Fig. 6 of the first shell of i-(Al-Mn) resembles that of i-(Al-Mn-Si) with a slight shift of the main peak position and a further smearing of the shoulder at smaller r. Note that the RDF of i-(Al-Mn) is also quite similar to the simulated RDF for Al_6Mn. This points out the fact that no unambiguous conclusion can be drawn based on the RDF of the first shell alone. Yet, as has been demonstrated, the analysis of the Mn-Mn shells permit conclusive results, taking advantage of the unique structure of α-(Al-Mn-Si). We have found that the MI with the average dimension given in Fig. 10 is the rigid unit in the IP, and these MI units are interconnected in a fashion such that about 40% of the connections resemble those in the α phase while the rest are more disordered.

No such detailed conclusions can be obtained for the decagonal phase. The first-shell RDF has a broader distribution than that of i-(Al-Mn). We also note in the Fourier transform (Fig. 4) that the peaks near 4.5–5 Å show different behavior than the ones in the IP's. The peak height is higher at around 4.5 Å than at 5 Å. The peak at 5 Å is much smaller than the one in i-(Al-Mn). We thus find no evidence for a structural unit in the decagonal phase similar to the one in the IP's. We note that a recent EXAFS study[30] found that Fe and Mn atoms occupy different sites in the decagonal Fe-Mn-Al alloys while they occupy similar sites in the IP, indicating a difference between the two. It is usually found that the decagonal phase is quite defective, which might have an effect on any interpretation.

We compare our results with the models for the interconnections of the units in the IP: (1) the centers of the units are located on a quasicrystalline array,[3,6] including the proposed phason strains to account for the observed finite correlation length for the IP; (2) the units are randomly connected along their threefold axes and maintain their orientation;[5,8,9,11] (3) the units are connected into cubic crystallites which are twinned to one another with icosahedral symmetry.[13] Our results are not in agreement with the current models of type (1) and (2). The main discrepancy is that the coordination numbers predicted by these models are too low, usually about 5 for QC models and 4 for the type (2) models. It is not clear to us that the QC models an accommodate the cubic environment, although the cubic packing can be regarded as a type of phason strain. On the other hand, it has been shown that the twinning model cannot explain the experimental results of transmission electron microscopy (TEM), x-ray, heat transformation, etc. The main problem with the twinning model is it postulates crystal sizes too large to be consistent with experimental results, including our own. When the crystal sizes become as small as our cubic correlation length, then they lose their identity as separate crystals as their intergrandular connections become an inherent part of the structure. We believe that the random packing model with some kind of short-range order, like the cubic order we found in this paper, is the better model for the IP. We note recently that Goldman and Stephens[31] have done some preliminary work in this direction. We have simulated the effects of the cubic regions in the icosahedral phase by putting small crystallites in the random packing model.[32] We found that the presence of microcrystallites in general broadens the diffraction peaks relative to an "ideal" random packing model in a manner toward better agreement with experimental observations. Furthermore, the packing density and connectivity are also improved.

The presence of the fine grains of the α phase in the icosahedral phase can be explained by considering the formation of the icosahedral phase. We assume that the melt is composed of MI units which are not oriented relative to one another so that they approximate hard spheres. Typical hard-sphere liquids have an average nearest-neighbor coordination number around 8. When the liquid solidifies, the orientational forces take hold to connect the units along the threefold icosahedral axes. The MI units can have at most eight such neighbors corresponding to bcc arrangement with the eight threefold axes so connected along the cubic [111] directions, leaving 12 threefold axes unconnected. Because of the fluctuations in the liquid and because there may be residual Al atoms between the units to block the attachment of the units, a significant number of the units will have fewer than eight neighbors in the solid, permitting them to connect differently from bcc packing along the threefold axes of the MI units. Thus the cubic symmetry is broken and the icosahedral symmetry prevails naturally through the symmetry of the units. We note that this discussion also provides a new method for the modeling of the icosahedral phase.

This work is done on the systems of Al-Mn and Al-Mn-Si. There is experimental evidence that a different type of unit occurs in the IP of Al-Cu-Li ($T2$ phase).[33,34] The possibility exists that the structure of other IP's may be different with different or no icosahedral units and different connections. It should be mentioned that the reason such accurate results can be obtained for the i-(Al-Mn-Si) is because the short-range order is very similar to that of the α phase.

VII. CONCLUSION

The unique structure of α-(Al-Mn-Si) is crucial for the success of our XAFS analysis. We have found that MI

units of average radius ≈ 4.8 Å with 12 Mn and 30 Al atoms on the surface and 12 Al atoms directly below Mn atoms as shown in Fig. 11 are the average structural units in the *i*-(Al-Mn) and *i*-(Al-Mn-Si). Each MI in the IP has about seven neighboring MI's, down from the eight in the α phase. The MI units are distorted similar to the distortions present in the α phase, suggesting that the packing of the MI units in the IP resemble to a large extent that in the α phase. The result also suggests that the identity of the two types of MI is also preserved in the IP. The results can be best explained by the presence of small cubic regions with a correlation length of about 20 Å in the IP. The more disordered connections between the MI units can be assigned to the intergranular regions between the cubic regions which are coherent parts of the structure. The results are inconsistent with all the current models of the IP, including the quasicrystalline and the random packing model for the IP. The random packing model needs to be modified to generate a larger coordination number for the structural units and to include the cubic regions. We suggest that the IP could be modeled by starting with the short-range order of the melt and orienting the MI units as the IP solidifies. This will necessarily generate much bcc environment in the structure. We also find that Si atoms have an effect on the connection between the structural units. We find no evidence for the MI as the structural unit in the decagonal Al-Mn phase.

Note added. During the revision process of this manuscript, we encountered related works by Cahn *et al.*[35] and Janot *et al.*[36] A Patterson analysis of the neutron and x-ray data for α- and *i*-(Al-Mn-Si) also demonstrated the similarity between the short-range structures of these two phases.[35] Partial pair correlation functions obtained from neutron scattering data[36] give results in good agreement with our EXAFS results presented here.

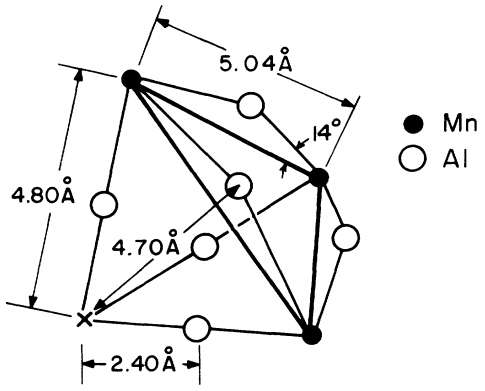

FIG. 11. The dimension of the Mackay icosahedral unit proposed for *i*-(Al-Mn-Si). One of the 20 icosahedral faces of the MI is shown. The center of the MI is empty and is marked *X*. The error bars in the distances are about 0.03 Å while the error bar in the angle is about 1°.

ACKNOWLEDGMENTS

We are most thankful for informative discussions with J. W. Cahn. We are grateful to J. W. Cahn, R. J. Schaefer, and D. Shechtman for supplying the samples used in the measurement. We thank C. E. Bouldin for assistance in the measurements and useful discussions, Jose Mustre and J. J. Rehr for discussion on the multiple-scattering effect, and D. Mastropolo for helping to generate Fig. 3. This work is supported in part by the U.S. Department of Energy under DE-A505-80-ER10742.

[1]D. Shechtman, I. Blech, D. Gratias, and J. W. Cahn, Phys. Rev. Lett. **53**, 1951 (1984).
[2]L. Bendersky, Phys. Rev. Lett. **55**, 1461 (1985).
[3]P. Guyot and M. Audier, Philos. Mag. B **52**, L15 (1985).
[4]V. Elser and C. L. Henley, Phys. Rev. Lett. **55**, 2883 (1985).
[5]Y. Ma, E. A. Stern, and C. E. Bouldin, Phys. Rev. Lett. **57**, 1611 (1986).
[6]D. Gratias and J. W. Cahn, J. Phys. (Paris) Colloq. **47**, C3-415 (1986).
[7]D. Levine and P. J. Steinhardt, Phys. Rev. Lett. **53**, 2477 (1984).
[8]D. Shechtman and I. Blech, Metall. Trans. **16A**, 1005 (1985).
[9]P. W. Stephens and A. I. Goldman, Phys. Rev. Lett. **56**, 1168 (1986).
[10]P. A. Bancel, P. A. Heiney, P. W. Stephens, A. I. Goldman, and D. M. Horn, Phys. Rev. Lett. **54**, 2422 (1985).
[11]E. A. Stern, Y. Ma, K. Bauer, and C. E. Bouldin, J. Phys. (Paris) Colloq. **47**, C3-371 (1986).
[12] T. C. Lubensky, J. E. S. Socolar, P. J. Steinhardt, P. A. Bancel, and P. A. Heiney, Phys. Rev. Lett. **57**, 1440 (1986); P. M. Horn, W. Malzfeldt, D. P. DiVincenzo, J. Toner, and R. Gambino, *ibid.* **57**, 1444 (1986).
[13]L. Pauling, Phys. Rev. Lett. **58**, 365 (1987).
[14]For a review see, e.g., E. A. Stern and S. M. Heald, in *Handbook on Synchrotron Radiation,* edited by D. E. Eastman, Y. Farge, and E. E. Koch (North-Holland, Amsterdam, 1980).
[15]E. A. Stern, Y. Ma, O. Henske-Petitpierr, and C. E. Bouldin (unpublished).
[16]M. Cooper and K. Robinson, Acta. Crystallogr. **20**, 614 (1966).
[17]C. L. Henley (private communication).
[18]B.-K. Teo, J. Am. Chem. Soc. **103**, 3990 (1981).
[19]A. D. I. Nicol, Acta. Crystallogr. **6**, 285 (1953).
[20]E. A. Stern, Y. Ma, and C. E. Bouldin, Phys. Rev. Lett. **55**, 2172 (1985).
[21]J. B. Boyce, J. C. Mikkelson, Jr., F. Bridges, and T. Egami, Phys. Rev. B **33**, 7314 (1986).
[22]M. A. Marcus, H. S. Chen, G. P. Espinosa, and C. L. Tsai, Solid State Commun. **58**, 227 (1985).
[23]A. Sadoc, A. M. Flank, P. Lagarde, P. Sainfort, and R. Bellisent, J. Phys. (Paris) **47**, 873 (1986).
[24]P. A. Heiney, P. A. Bancel, A. I. Goldman, and P. W. Stephens, Phys. Rev. B **34**, 6746 (1986).
[25]B.-K. Teo and P. A. Lee, J. Am. Chem. Soc. **101**, 2815 (1979).
[26]G. B. Bunker and E. A. Stern, Phys. Rev. Lett. **52**, 1990 (1984).

[27]J. Mustre and J. J. Rehr (unpublished).
[28]E. A. Stern and Y. Ma, Philos. Mag. Lett. **56**, 103 (1987).
[29]M. Wilkens (private communication).
[30]Y. Ma and E. A. Stern, Phys. Rev. B **35**, 2678 (1987).
[31]A. I. Goldman and P. W. Stephens (unpublished); P. M. Horn *et al.* (unpublished).
[32]Y. Ma and E. A. Stern (unpublished); Y. Ma, Ph.D. thesis, University of Washington, 1987.
[33]Y. Ma, E. A. Stern, and F. W. Gayle, Phys. Rev. Lett. **58**, 1956 (1987).
[34]M. Audier, P. Sainfort, and B. Dubois, Philos. Mag. B **54**, L105 (1986).
[35]J. W. Cahn, D. Gratias, and B. Mozer, Phys. Rev. B (to be published).
[36]C. Janot, J. Dubois, and J. Pannetier, Physica B + C **146B**, 351 (1987).